The Plant Cell, Vol. 19: 2186–2196, July 2007, www.plantcell.org

Ethylene Upregulates Auxin Biosynthesis in *Arabidopsis* Seedlings to Enhance Inhibition of Root Cell Elongation [W]

Ranjan Swarup,[a] Paula Perry,[a,b,c] Dik Hagenbeek,[d] Dominique Van Der Straeten,[d] Gerrit T.S. Beemster,[b,c] Göran Sandberg,[e] Rishikesh Bhalerao,[f] Karin Ljung,[f] and Malcolm J. Bennett[a,1]

[a] School of Biosciences and Centre for Plant Integrative Biology, University of Nottingham, LE12 5RD Nottingham, United Kingdom

[b] Department of Plant Systems Biology, Flanders Institute for Biotechnology, B-9052, Ghent, Belgium

[c] Department of Molecular Genetics, Ghent University, B-9052 Ghent, Belgium

[d] Department of Molecular Genetics, Plant Hormone Signaling and Bio-imaging, Ghent University, B-9000 Ghent, Belgium

[e] Department of Plant Physiology, Umeå Plant Science Centre, Umeå University, SE-901 87 Umeå, Sweden

[f] Department of Forest Genetics and Plant Physiology, Umeå Plant Science Centre, Sveriges Lantbruksuniversitet, SE-901 83 Umeå, Sweden

Ethylene represents an important regulatory signal for root development. Genetic studies in *Arabidopsis thaliana* have demonstrated that ethylene inhibition of root growth involves another hormone signal, auxin. This study investigated why auxin was required by ethylene to regulate root growth. We initially observed that ethylene positively controls auxin biosynthesis in the root apex. We subsequently demonstrated that ethylene-regulated root growth is dependent on (1) the transport of auxin from the root apex via the lateral root cap and (2) auxin responses occurring in multiple elongation zone tissues. Detailed growth studies revealed that the ability of the ethylene precursor 1-aminocyclopropane-1-carboxylic acid to inhibit root cell elongation was significantly enhanced in the presence of auxin. We conclude that by upregulating auxin biosynthesis, ethylene facilitates its ability to inhibit root cell expansion.

INTRODUCTION

Ethylene represents a key regulatory signal in higher plants (reviewed in Smalle and Van Der Straeten, 1997; Alonso and Stepanova, 2004). This volatile hydrocarbon molecule (C_2H_4) is best known for triggering fruit ripening (reviewed in Chaves and de Mello-Farias, 2006), but it also plays a crucial role during root development (reviewed in Hussain and Roberts, 2002). Blocking ethylene synthesis or signaling disrupts the ability of tomato (*Solanum lycopersicum*) roots to penetrate compact soil or even loose sand (Clark et al., 1999; Hussain et al., 1999). In *Arabidopsis thaliana* roots, ethylene and its precursor 1-aminocyclopropane-1-carboxylic acid (ACC) have been described to cause three growth responses: the induction of ectopic root hairs (Tanimoto et al., 1995; Masucci and Schiefelbein, 1996), an increase in the width of the root (Smalle and Van Der Straeten, 1997), and a rapid but reversible downregulation of cell elongation (Le et al., 2001). These three ethylene-induced adaptive responses will confer greater anchorage, aid soil penetration, and provide more dynamic regulation of root growth, respectively.

[1] Address correspondence to malcolm.bennett@nottingham.ac.uk.
The author responsible for distribution of materials integral to the findings presented in this article in accordance with the policy described in the Instructions for Authors (www.plantcell.org) is: Malcolm J. Bennett (malcolm.bennett@nottingham.ac.uk).
[W] Online version contains Web-only data.
www.plantcell.org/cgi/doi/10.1105/tpc.107.052100

Great advances in our knowledge about the molecular basis of ethylene action have been made in the last decade employing genetic approaches in *Arabidopsis* (reviewed in Alonso and Stepanova, 2004). The isolation of a series of ethylene response mutants led to the identification of a number of key signal transduction components. ETR1 encodes a histidine kinase-like receptor protein that mediates ethylene perception (Chang et al., 1993). ETR1 and its related proteins directly regulate the activity of the Raf-like kinase protein CTR1, which functions to repress ethylene signaling (Kieber et al., 1993). Ethylene binding to ETR1 causes inactivation of CTR1 (Clark et al., 1998), releasing the repression of EIN2, resulting in the upregulation of expression of downstream genes by the transcription factor, EIN3.

Intriguingly, mutations in many auxin transport or signaling components also cause aberrant responses to ethylene, indicating crosstalk between these two growth regulators (Pickett et al., 1990; Roman et al., 1995; Luschnig et al., 1998; Rahman et al., 2001; Stepanova et al., 2005; Chilley et al., 2006). For example, mutations in the auxin influx and efflux carrier genes *AUX1* and *EIR1*/*AGR*/*PIN2* (Pickett et al., 1990; Luschnig et al., 1998; henceforth referred to as *PIN2*) and the auxin receptor *TIR1* (Alonso et al., 2003) confer ethylene-insensitive root growth phenotypes. Stepanova et al. (2005) recently demonstrated that mutations in two *Arabidopsis* genes (*ASA1* and *ASB1*), encoding subunits of the anthranilate synthase enzyme, which synthesizes an auxin precursor, also confer ethylene-insensitive root growth phenotypes. Epistasis studies have positioned these auxin signaling components downstream of the ethylene signal transduction pathway (Roman et al., 1995; Stepanova et al., 2005),

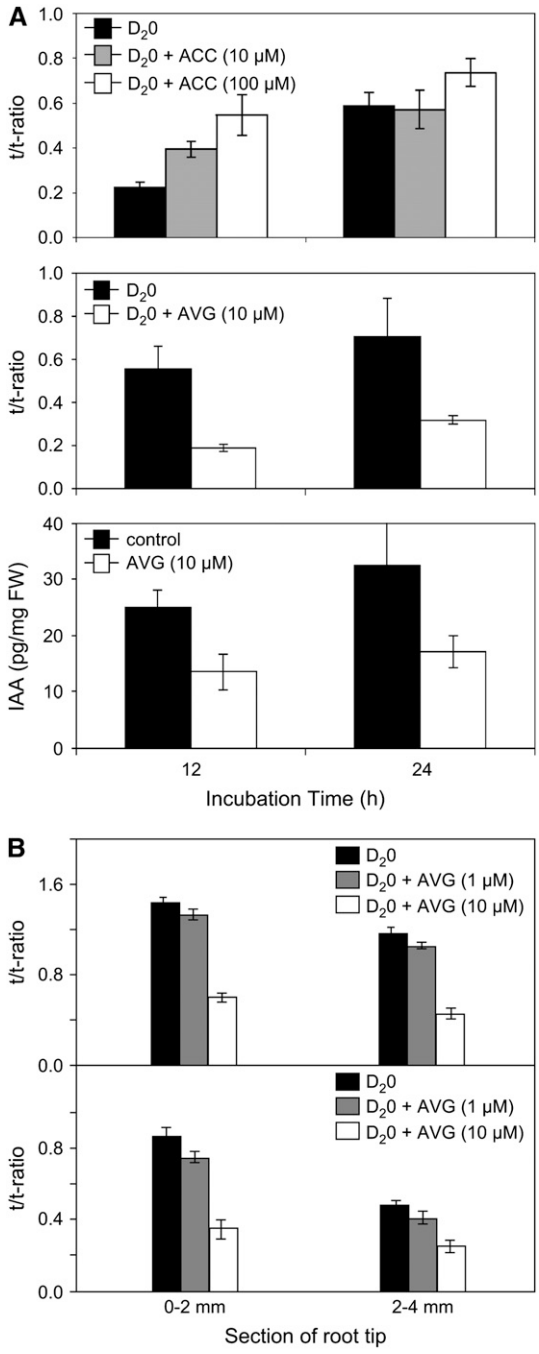

Figure 1. Manipulating Ethylene Synthesis in *Arabidopsis* Seedlings Also Alters the Synthesis and Abundance of Auxin.

(A) IAA synthesis and abundance was measured in 6-d-old *Arabidopsis* seedlings that were incubated for 12 and 24 h with D_2O medium containing the ethylene precursor ACC (top panel) or the ethylene synthesis inhibitor AVG (middle panel). IAA abundance was measured in 6-d-old *Arabidopsis* seedlings that were incubated for 12 and 24 h with D_2O medium containing AVG (bottom panel). FW, fresh weight.

(B) IAA synthesis was measured in 6-d-old *Arabidopsis* seedling roots treated with the ethylene synthesis inhibitor AVG. After 6 d of growth, either whole seedlings (top panel) or excised roots (bottom panel) were fed with D_2O medium containing AVG for 24 h. IAA synthesis was measured in 2-mm segments of wild-type *Arabidopsis* roots sampled from tissues 0 to 2 mm and 2 to 4 mm from the apex. After correction for natural isotope abundances, ratios between the labeled tracer (mass-to-charge ratio [m/z] of 203, 204, and 205) and unlabeled tracee (m/z 202) were calculated for IAA (expressed as the t/t-ratio).

suggesting that ethylene inhibition of root growth requires auxin biosynthesis, transport, and responses.

This study aims to understand the requirement for auxin during ethylene-regulated root growth. Initially employing mass spectrometry, we determined that ethylene positively controls auxin biosynthesis in the root apex. Targeted expression experiments revealed that ethylene requires auxin to be transported from the root apex to elongation zone tissues to inhibit root growth. Kinematic growth measurements revealed that inhibition of root cell elongation by ethylene was significantly enhanced in the presence of auxin. We conclude that ethylene upregulates auxin biosynthesis to maximize its ability to inhibit root cell expansion.

RESULTS

Ethylene Positively Regulates Auxin Biosynthesis in *Arabidopsis* Roots

Recent genetic evidence suggests that ethylene mediates its growth inhibitory effects in *Arabidopsis* roots by regulating auxin synthesis (Stepanova et al., 2005). We directly measured whether ethylene upregulated auxin synthesis employing a mass spectrometry–based assay (Ljung et al., 2005; see Methods).

We initially investigated whether manipulating ethylene in *Arabidopsis* seedling tissues impacted the rate of indole-3-acetic acid (IAA) synthesis. Six-day-old intact seedlings were incubated for 12 or 24 h in liquid medium containing 30% D_2O (^2H_2O). Inclusion of the ethylene biosynthetic precursor ACC into the liquid medium resulted in a significant increase in the rate of IAA synthesis (versus the untreated control) within 12 h (top panel, Figure 1A). Treatment with 10 μM ACC doubled the rate of IAA synthesis, while 100 μM ACC resulted in a threefold increase. Conversely, inclusion of the (ACC synthase) inhibitor 1-aminoethoxyvinyl-glycine (AVG) into the liquid medium resulted in a significant decrease in the rate of IAA synthesis (versus the untreated control; middle panel, Figure 1A). After 12- and 24-h treatments, 10 μM AVG reduced IAA synthesis by ~60 and 50%, respectively. Parallel measurements of auxin abundance in these samples detected comparable changes in IAA concentration (bottom panel, Figure 1A; see Methods). Our mass spectrometry measurements therefore reveal that manipulating the levels of ethylene synthesis in *Arabidopsis* seedling tissues also impacts IAA biosynthesis, which result in equivalent changes in IAA levels.

We next addressed whether IAA synthesis in root tissues was also regulated by ethylene. High levels of newly synthesized IAA were observed in root apical tissues after 6-d-old intact seedlings were incubated in liquid medium containing 30% D_2O (top panel, Figure 1B). Significant incorporation of deuterium into IAA

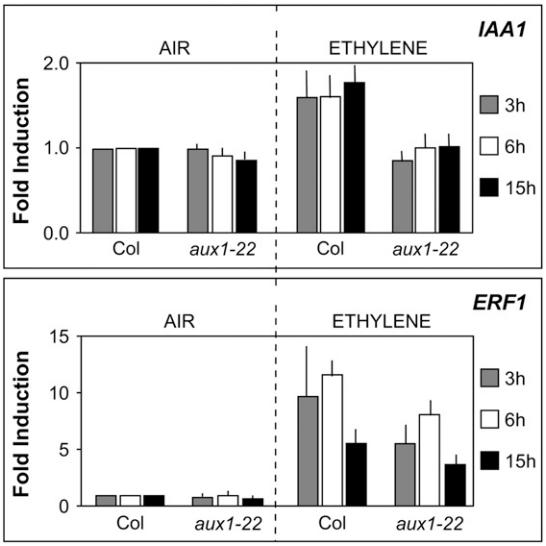

Figure 2. *aux1* Blocks the Induction of Auxin (but Not Ethylene) Responsive Gene Expression after Ethylene Treatment.

Transcript abundance of the auxin-responsive gene *IAA1* (Abel and Theologis, 1995) and ethylene-responsive gene *ERF1* (Solano et al., 1998) was measured employing qRT-PCR. RNA was extracted from 10-d-old wild-type and *aux1-22* seedling roots 3, 6, and 15 h after treatment with ethylene (2 ppm) or ethylene-free air (controls). Data represent the average of three biological repeats (±SE). All values are normalized to that of Col-0 exposed to ethylene-free air for the same time period.

was also detected in root apices of whole excised roots (bottom panel, Figure 1B), consistent with roots having the capacity for de novo IAA biosynthesis. However, inclusion of 10 μM AVG in the liquid medium resulted in an ~50% decrease in the rates of IAA synthesis in root apices isolated from either intact seedlings or whole excised roots (Figure 1B). The highest level of IAA biosynthesis in the untreated control was observed in the most apical 2-mm root section isolated from either intact plants or whole excised roots (Figure 1B). IAA synthesis in this region of the root was also most affected by AVG treatment (Figure 1B). Gas chromatography selective reaction monitoring mass spectrometry measurements therefore demonstrate that ethylene upregulates IAA biosynthesis in *Arabidopsis* root apical tissues.

Ethylene Enhances Auxin-Responsive Gene Expression in Roots

Next, we monitored the effect of ethylene upregulating IAA biosynthesis in root tissues on auxin-responsive gene expression. Quantitative RT-PCR (qRT-PCR) assays (Figure 2) revealed that ethylene treatment upregulated the expression of the auxin-responsive gene *IAA1* (Abel and Theologis, 1995). Similar effects were observed employing the auxin-responsive reporter $IAA2_{pro}$*:*β*-glucuronidase* (*GUS*) (Luschnig et al., 1998; Swarup et al., 2001). In untreated wild-type roots, $IAA2_{pro}$*:GUS* was strongly expressed in the stele and columella but only weakly detected in lateral root cap and epidermal cells (Figure 3A). Following ethylene treatment of wild-type roots, $IAA2_{pro}$*:GUS* was also strongly expressed in the lateral root cap, older meristematic cells, and newly expanding cells (Figure 3F; see Supplemental Figure 1 online).

To determine whether changes in auxin-responsive gene expression are proportionate with ethylene signal transduction activity in root tissues, we monitored $IAA2_{pro}$*:GUS* expression in a variety of ethylene response mutant backgrounds. Mutations in the RAF-like kinase gene *CTR1* cause a constitutive ethylene response, resulting in inhibition of root growth even in the absence of ethylene (Kieber et al., 1993). We observed that *ctr1* mutant seedling roots exhibited increased levels of $IAA2_{pro}$*:GUS*

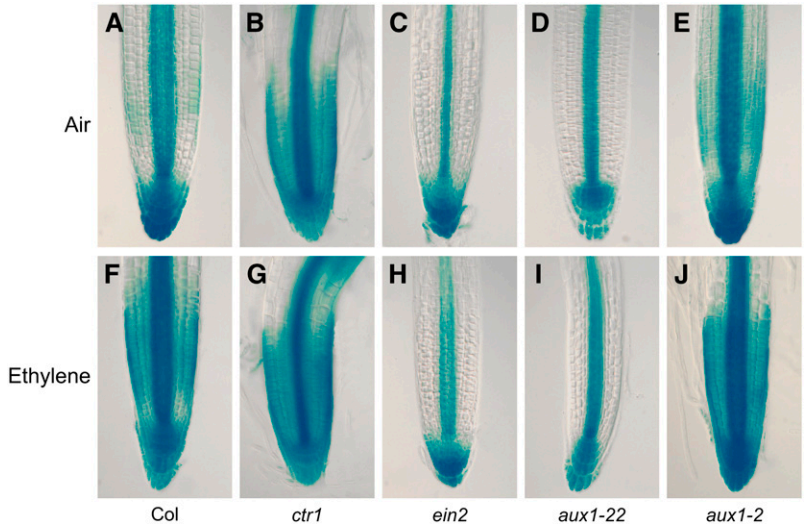

Figure 3. Induction of the Auxin-Responsive Reporter $IAA2_{pro}$*:GUS* by Ethylene Is Dependent on EIN2 and AUX1.

The expression of the $IAA2_{pro}$*:GUS* reporter was monitored in the wild type (**[A]** and **[F]**), in the constitutive ethylene response mutant *ctr1* (**[B]** and **[G]**), in the ethylene-insensitive mutant *ein2* (**[C]** and **[H]**), in the auxin influx carrier null allele *aux1-22* (**[D]** and **[I]**), and in the partial loss-of-function allele *aux1-2* (**[E]** and **[J]**). Seedlings were either grown in air (**[A]** to **[E]**) or in the presence of 10 μL/L of ethylene (**[F]** to **[J]**).

expression at the apex (Figures 3B and 3G) and throughout their mature tissues (see Supplemental Figure 1 online) in both air-grown and ethylene-treated samples. The pattern of $IAA2_{pro}$:*GUS* expression in *ctr1* roots phenocopied ethylene-treated wild-type roots (Figure 3F; see Supplemental Figure 1 online). $IAA2_{pro}$:*GUS* expression was also monitored in the ethylene-insensitive *ein2* mutant background. The air-grown *ein2* mutant exhibited a lower basal level of $IAA2_{pro}$:*GUS* root expression compared with the wild type (cf. Figures 3A and 3C). Ethylene treatment did not change the pattern of $IAA2_{pro}$:*GUS* spatial expression in the *ein2* mutant background compared with the ethylene-treated wild type (cf. Figures 3H and 3F). Hence, auxin-responsive gene expression in roots appears to be closely correlated with the ethylene signal transduction activity of the genetic background.

Ethylene-Mediated Inhibition of Root Growth Is Dependent on Auxin Transport

The changes in auxin-responsive reporter expression observed in ethylene mutant backgrounds and in the wild type following ethylene treatment may result from the upregulation of auxin biosynthesis throughout root apical tissues. Alternatively, like for root gravitropism, ethylene could cause auxin to accumulate at the root apex and then be transported back to the elongation zone by the auxin influx carrier AUX1 (Swarup et al., 2005). To

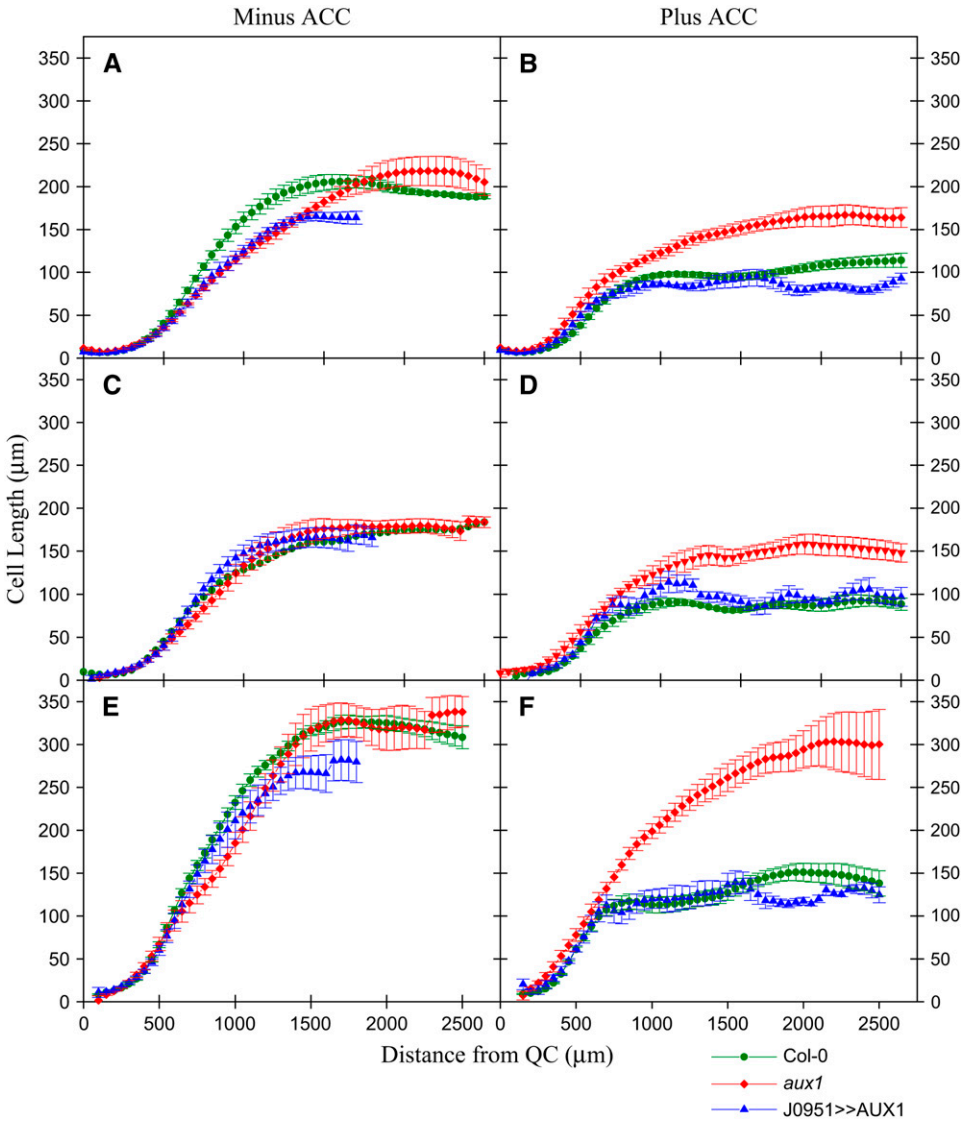

Figure 4. Inhibition of Root Cell Elongation by ACC Is Dependent on AUX1.

Profiles of cortical (**[A]** and **[B]**), epidermal trichoblast (**[C]** and **[D]**), and atrichoblast (**[E]** and **[F]**) cell expansion in wild-type (circles), *aux1* (diamonds), and *aux1 J0951≫AUX1* (triangles) roots. Seedlings were either grown in the absence (**[A]**, **[C]**, and **[E]**) or in the presence (**[B]**, **[D]**, and **[F]**) of 1 μM ACC. Cell lengths were measured relative to the quiescent center (QC) at the root apex using confocal microscopy (see Methods).

discriminate between these possibilities, we monitored the spatial expression of the *IAA2*$_{pro}$*:GUS* reporter in the *aux1* mutant background. In the case of the *aux1-22* null allele, no increase in reporter expression was observed in either lateral root cap or elongation zone tissues following ethylene treatment (Figure 3I). The inability of ethylene to modify reporter expression in an *aux1-22* background is unlikely to result from this allele blocking the ethylene sensitivity of root tissues. qRT-PCR assays revealed that ethylene was still able to induce the expression of the ethylene-responsive gene *ERF1* (Solano et al., 1998) in the *aux1-22* mutant background (Figure 2). Instead, *aux1-22* selectively blocked the upregulation of the auxin-responsive genes *IAA1* (Figure 2) and *IAA2* (Figure 3I). These altered patterns of gene expression are therefore consistent with *aux1* blocking the redistribution of ethylene-induced auxin accumulating at the root apex.

The functional importance of the AUX1-mediated redistribution of ethylene-induced IAA to root growth is further demonstrated by the ethylene insensitivity of the *aux1-22* allele (Roman et al., 1995). By contrast, the partial loss-of-function allele *aux1-2* (Swarup et al., 2004) exhibits ethylene-sensitive root growth (see Supplemental Figure 2 online), suggesting that sufficient auxin is still able to reach elongation zone tissues to block cell elongation. Consistent with this model, ethylene-treated *aux1-2* roots exhibit strong *IAA2*$_{pro}$*:GUS* expression in elongation zone tissues (Figure 3J). Hence, AUX1 is required for ethylene-mediated inhibition of root growth.

Inhibition of Root Cell Elongation by Ethylene Is Dependent on Auxin

Ethylene has been reported to inhibit root growth by reducing cell elongation (Le et al., 2001). Our mutant and reporter studies suggest that inhibition of root growth by ethylene is dependent on auxin transport from the root apex to elongation zone tissues. We tested whether auxin is required for ethylene inhibition of root cell elongation by performing detailed growth measurements on wild-type and *aux1* roots grown in the presence of the ethylene precursor ACC.

Confocal microscopy was used to measure changes in cell length profiles along the root axis induced by the presence of ACC (Figure 4). ACC (1 μM) was used for our growth studies because this concentration was observed to reduce root growth of wild-type plants by 50% (cf. Figures 4A and 4B). Measurements of wild-type epidermal (trichoblast and atrichoblast) and cortical cells revealed that the growth inhibition caused by 1 μM ACC correlated with a ~50% reduction in mature cell length (Figure 4). In the case of *aux1* roots, 1 μM ACC inhibited mature length of cells from these same tissues by ~20% (Figure 4). However, we were able to fully restore the sensitivity of *aux1* root cell elongation toward ACC in all cell types investigated by expressing AUX1 in mutant lateral root cap and epidermal tissues (termed line *aux1* J0951≫AUX1; Swarup et al., 2005). Hence, ethylene is able to partially inhibit root cell elongation in the absence of AUX1. However, full inhibition of root cell

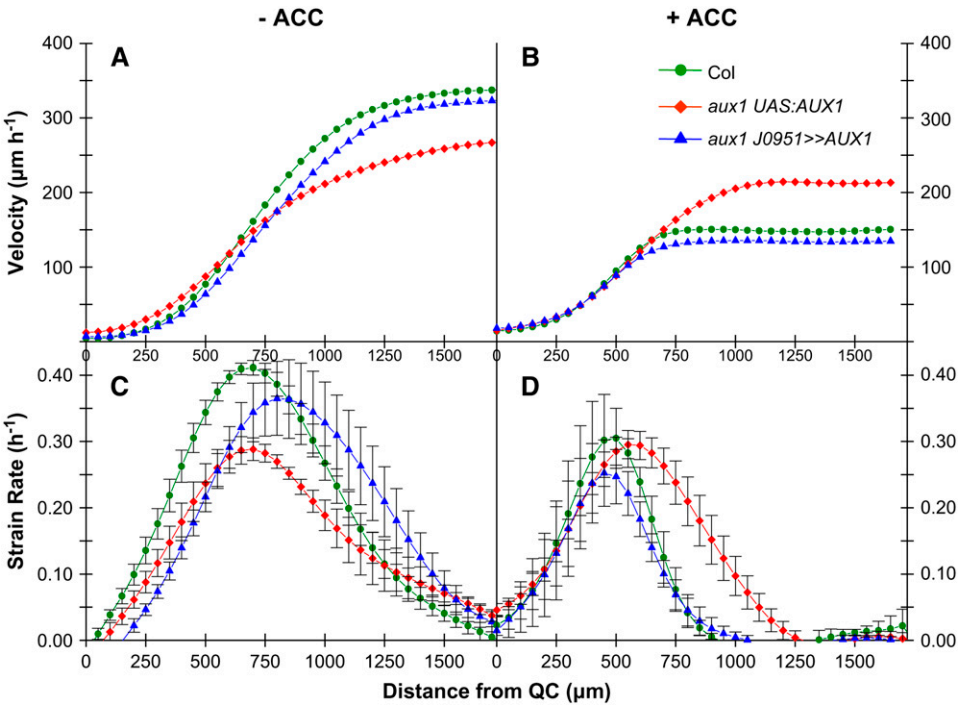

Figure 5. Kinematic Analysis of Root Growth Reveals That ACC Inhibits Rapid Cell Expansion.

Profiles of velocity (**[A]** and **[B]**) and relative rates of cell expansion (**[C]** and **[D]**) along the root elongation zones of the wild type (circles), *aux1* (diamonds), and *aux1 J0951≫AUX1* (triangles) were obtained from kinematic analysis. Seedlings were grown either in the absence (**[A]** and **[C]**) or in the presence (**[B]** and **[D]**) of 1 μM ACC.

expansion by ethylene appears to be dependent on AUX1-mediated transport of auxin from root apical to elongation zone tissues.

We next employed kinematic analysis to examine the impact of the inhibition of cell elongation by ACC on the dynamics of cell expansion in the same roots. This approach provides a detailed profile of the parameters that influence root growth rate (Beemster and Baskin, 1998). Figure 5A shows the velocity profile of untreated control roots. The velocity typically increases slowly near the root tip and then increases much more rapidly when cell division ceases and reaches a maximum when the root cells are fully expanded (Figure 5A; Beemster and Baskin, 2000). Kinematic measurements revealed that 1 μM ACC caused ~50% reduction in wild-type growth rate (Figure 5B). By contrast, ACC had only a small effect (~20%) on the growth rate of *aux1* roots. However, we were able to fully restore the sensitivity of *aux1* root growth toward ACC in line *aux1* J0951≫AUX1 (Figure 5B; Swarup et al., 2005).

Figures 5C and 5D show the derivative of the velocity profile, which gives the relative elongation rate, which is also termed the strain rate (Beemster and Baskin, 2000). ACC had no significant effect on cell expansion rates in the apical 500 μm of the root, roughly corresponding to the meristem (Beemster and Baskin, 1998). By contrast, the expansion rates in the region of rapid cell expansion are markedly affected by the treatment, consistent with the target of ethylene inhibition being cell expansion. In control roots, elongation continues until ~1700 μm from the apex of the root and maximum strain rates are ~0.40 h^{-1} (Figure 5C). The strain rate in wild-type and *aux1* J0951≫AUX1 roots grown in ACC shows that growth inhibition is due to a reduction in the length of the elongation zone to <1000 μm and an inhibition of maximum strain rates to ~0.30 h^{-1} (Figure 5D). By contrast, the strain rate of *aux1* roots grown in ACC is less affected, with elongation occurring over 1250 μm from the apex of the root, and maximum strain rates that were reduced to 0.30 h^{-1} by the *aux1* mutation were not reduced further by ACC (Figure 5D). We conclude that inhibition of root cell expansion by ethylene is due to a reduction in the size of the elongation zone and on maximum expansion rates that are dependent on AUX1-mediated transport of auxin from root apical to elongation zone tissues.

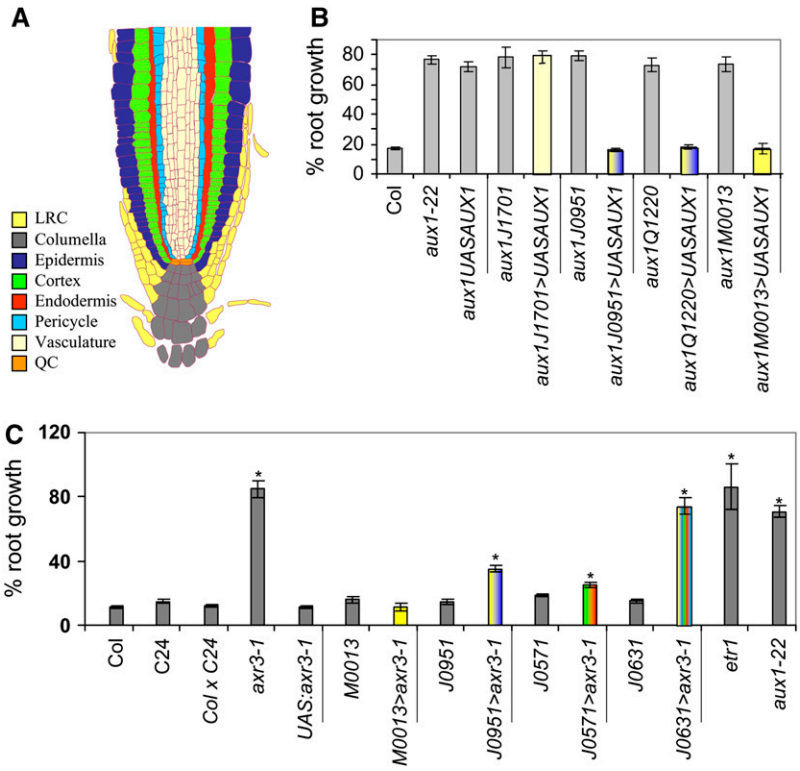

Figure 6. Ethylene-Inhibited Root Growth Is Dependent on Auxin Transport and Responses.

(A) Schematic diagram summarizing *Arabidopsis* root apical tissue organization. LRC, lateral root cap; QC, quiescent center.

(B) The sensitivity of *aux1* root growth toward ethylene could be restored by targeting the expression of AUX1 in elongating epidermal and/or the lateral root cap cells in the *aux1 J0951≫AUX1*, *aux1 Q1220≫AUX1*, and *aux1 M0013≫AUX1* lines, respectively.

(C) The sensitivity of wild-type root growth toward ethylene could be partially disrupted by targeting the expression of axr3-1 in cortical/endodermal or epidermal cells in the *J0951≫axr3-1* and *J0571≫axr3-1* lines, respectively. Strong ethylene resistance was observed in the *J0631≫axr3-1* line, which expresses axr3-1 in every elongation zone tissue. Seedlings were grown vertically on Murashige and Skoog (MS) plates either in air or ethylene (10 μL/L) for 5 d. Root growth in the presence or absence of ethylene was measured and expressed as a percentage of root growth compared with the air control. Asterisks indicate significant difference from the control ($P < 0.05$; see Supplemental Figure 5 online for further details). The color coding of bars either refers to the root tissues in which either AUX1 or axr3-1 expression is targeted or, if black, denotes them as controls. The *aux1-22*, *etr1-1*, and *axr3-1* mutants represent ethylene-resistant controls.

Ethylene Inhibition of Root Growth Is Dependent on Auxin Responses in Multiple Elongation Zone Tissues

We next investigated whether ethylene inhibition of root growth, like root gravitropism (Swarup et al., 2005), requires AUX1 to accumulate IAA in expanding epidermal cells. We addressed this question by employing a number of *aux1* lines expressing AUX1 in subsets of tissues within its root expression domain (Swarup et al., 2005). Intriguingly, we observed that AUX1 did not require to be expressed in *aux1* epidermal cells to rescue the mutant's sensitivity toward ethylene (Figure 6B). Instead, AUX1 expression in lateral root cap cells (*M0013≫AUX1*) was sufficient to result in inhibition of *aux1* root growth by ethylene (Figure 6B). This result suggests that, unlike gravitropism (Swarup et al., 2005), inhibition of root growth by ethylene does not depend on AUX1 accumulating IAA in expanding epidermal cells.

To determine which elongation zone tissues are required to respond to the ethylene-induced auxin signal, we targeted the expression of the mutant auxin repressor protein axr3-1 in selected root tissues employing a selection of GAL4 driver lines (Swarup et al., 2005; see Supplemental Figure 3 online). Only weak resistance toward ethylene was conferred when targeting the expression of axr3-1 in either the root epidermis (*J0951≫axr3-1*; Figure 6C), epidermal and cortical (*J2812≫axr3-1* and *Q2393≫axr3-1*; see Supplemental Figure 4 online), or cortex and endodermis (*J0571≫axr3-1*; Figure 6C). However, strong ethylene resistance equivalent to the *axr3-1* mutant itself was only obtained when targeting axr3-1 expression to every elongation zone tissue (*J0631≫axr3*-1; Figure 6C). Our results suggest that ethylene inhibition of root growth is dependent on auxin acting on multiple elongation zone tissues simultaneously.

Many auxin response mutants have been reported to exhibit ethylene-insensitive root growth phenotypes (reviewed in Swarup et al., 2002). We employed the $IAA2_{pro}$*:GUS* reporter to monitor auxin-responsive gene expression in the *axr1*, *axr2*, *axr3*, and *axr4* mutant backgrounds following ethylene treatment. We observed no change in reporter expression in the root apical tissues of the ethylene-resistant mutant *axr2-1* (Wilson et al., 1990) and *axr3-1* (Leyser et al., 1996) following ethylene treatment (Figures 7H and 7I). This contrasted with the strong upregulation of the $IAA2_{pro}$*:GUS* reporter in root tissues of the ethylene-sensitive wild-type and *axr4* lines (Figures 7F and 7J; Hobbie and Estelle, 1995) and, to a lesser extent, in the weakly ethylene-resistant mutant background *axr1-12* (Figure 7G; Timpte et al., 1995). Therefore, the level of auxin-responsive gene expression in root apical tissues appears to be closely correlated with the ethylene sensitivity of the genetic background.

DISCUSSION

Ethylene-Regulated Root Growth Is Dependent on Auxin Biosynthetic, Transport, and Response Proteins That Function in Distinct Tissues

The genetic dissection of ethylene-regulated *Arabidopsis* root growth has identified a large number of genes encoding proteins with either ethylene or auxin-related functions (reviewed in Swarup et al., 2002; Stepanova and Alonso, 2005). Epistasis experiments have enabled first ethylene and then auxin-related gene products to be positioned relative to one another in a signal transduction pathway (Roman et al., 1995; Stepanova et al., 2005). While such studies have helped reveal the sequence of events at the molecular level, they do not convey information about the spatial organization of the transduction pathway in which these proteins function.

Our study has revealed that the auxin biosynthetic, transport, and response proteins that function in this signaling pathway

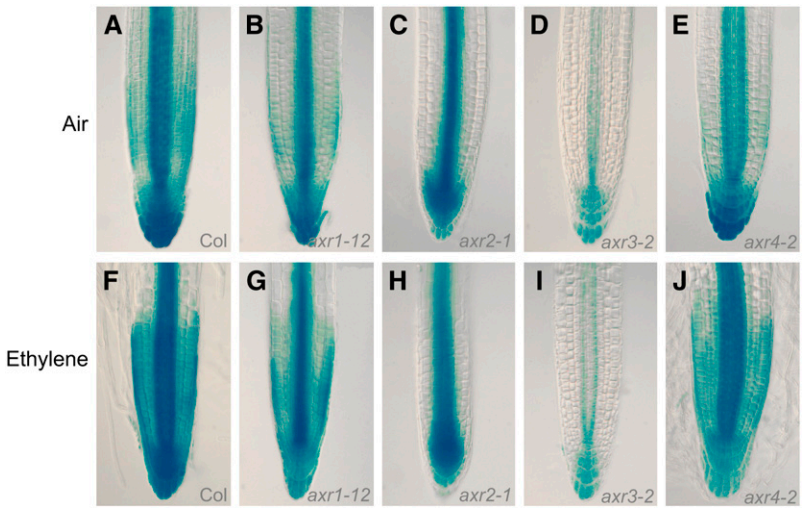

Figure 7. Induction of $IAA2_{pro}$*:GUS* by Ethylene Is Blocked by *axr2-1* and *axr3-1*.

The expression of the $IAA2_{pro}$*:GUS* reporter was monitored in a variety of auxin response mutant backgrounds either grown in air (**[A]** to **[E]**) or after ethylene treatment (10 μL/L; **[F]** to **[J]**).

operate in distinct root apical tissues. Mass spectrometry measurements have determined that the highest level of ethylene-regulated IAA biosynthesis is detected at the root tip (Figure 1B). Several *Arabidopsis* genes encoding enzymes involved in IAA biosynthesis are expressed at the root apex (Ljung et al., 2005; Stepanova et al., 2005). Ethylene has been observed to upregulate the expression of at least two of these genes (*ASA1* and *ASB1*; Stepanova et al., 2005). Based on these observations, we have positioned the site of ethylene-regulated IAA biosynthesis at the root apex (Figure 8).

Auxin transport is also required for ethylene-mediated inhibition of root growth. The auxin influx carrier AUX1 (Yang et al., 2006) and auxin efflux carrier PIN2 (Wisniewska et al., 2006) are essential for mobilizing IAA between root apical and elongation zone tissues (Figure 3; Růžička et al., 2007). Parallels can be drawn with root gravitropism where AUX1 and PIN2 expression is required in lateral root cap and epidermal cells to mobilize IAA from the root apex (Swarup et al., 2005). However, this study has revealed that, at least in the case of AUX1, the auxin influx carrier is only required to be expressed in lateral root cap cells to restore the ethylene sensitivity of *aux1* roots. This observation helps explain why *axr4* exhibits an ethylene-sensitive root growth phenotype (Hobbie and Estelle, 1995) since this mutation selectively disrupts trafficking of AUX1 to the plasma membranes of epidermal but not lateral root cap cells (Dharmasiri et al., 2006). Based on our observations, we have positioned AUX1 in lateral root cap cells (Figure 8).

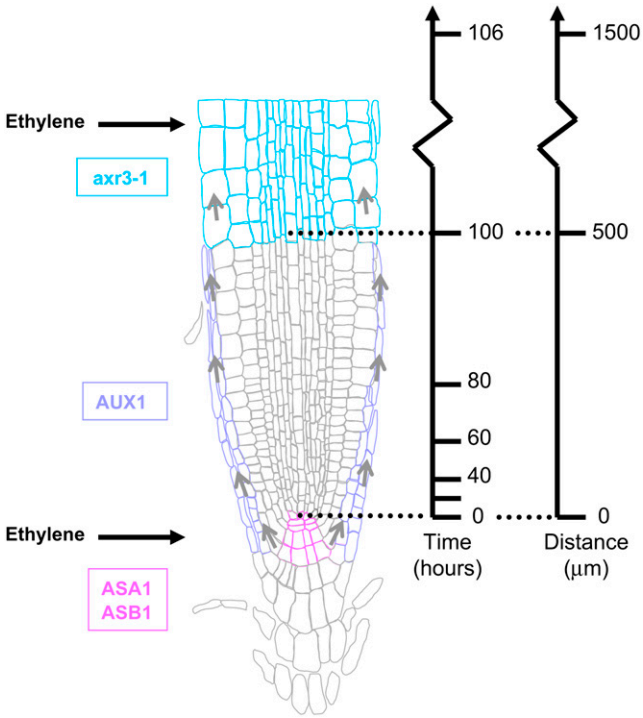

Figure 8. Model for Auxin Action during Ethylene-Regulated Root Growth.

The model provides a spatial framework on which to place auxin components required for ethylene responses in roots. The schematic diagram of the *Arabidopsis* root apex is overlaid with the sites of action of auxin biosynthesis (WEI2/ASA1 and WEI7/ASB1) and transport (AUX1) components required for ethylene inhibition of root growth. Small arrows denote the basipetal flow of auxin from the root apex via the lateral root cap to the elongation zone. Sites of ethylene-responsive gene expression are denoted by large horizontal arrows. We also highlight that the dominant gain-of-function mutation *axr3-1/iaa17* can disrupt ethylene inhibition of root growth in elongation zone tissues. Vertical arrows either represent the time required or distance moved by root cells as they progress through meristematic and elongation zones.

Selected components of the auxin response machinery are also required for ethylene inhibition of root growth. For example, the auxin receptor mutant *tir1* (Růžička et al., 2007; Stepanova et al., 2007) and auxin response mutants *axr2-1* (Wilson et al., 1990) and *axr3-1* (Leyser et al., 1996; Figure 6C) confer an ethylene-insensitive root growth phenotype. Targeted expression studies performed in this study have revealed that multiple elongation zone tissues must express axr3-1 to confer an ethylene-resistant root growth phenotype (Figure 6). This contrasts with auxin-resistant and agravitropic root growth phenotypes that can be engineered by expressing axr3-1 in elongating epidermal cells (Swarup et al., 2005). Hence, we have positioned AXR3/IAA17 in the elongation zone tissues (Figure 8). We conclude that ethylene inhibition of root growth requires auxin responses in multiple elongation zone tissues.

Ethylene Inhibits the Most Rapid Phase of Cell Expansion in Roots

We recognize that temporal, as well as spatial, aspects of the root growth response to ethylene also need to be taken into consideration. Le et al. (2001) elegantly demonstrated that the inhibitory effect of ethylene on root elongation occurs within minutes after application. It is often overlooked that the time axis along the root is strongly skewed: Cells undergoing rapid postmeristematic expansion make up the bulk of the length of the growth zone, which suggests that this part of their development would take a relatively long period of time. Interestingly, due to the much higher velocity at which cells move along the elongation zone than in the more apical regions, postmeristematic expansion takes only a few hours to complete, whereas cells spend several days to traverse the meristem (see time axis in Figure 8; Beemster and Baskin, 1998).

Kinematic analysis has allowed us to pinpoint the precise location in the root growth zone where ethylene exerts its effect. It is intriguing to see that cell expansion rates are completely insensitive to ethylene in the first 500 μm from the quiescent center. Comparison with kinematic analysis of cell division rates (Beemster and Baskin, 1998) showed that the zone of cell division ends where wild-type cells reach two-thirds of their maximum rate of cell expansion. The data presented here clearly demonstrate that it is precisely at this position where the effect of ethylene on expansion is first observed (Figure 6). This implies that ethylene specifically inhibits growth of expanding but not dividing cells. Root hairs are initiated at the position where cell expansion rates are maximal (Le et al., 2001). Our kinematic data clearly shows that ethylene inhibition of cell expansion moves

this maximum to a more apical position (Figure 5). This is consistent with the macroscopic observation that the root hair zone also rapidly moves to a position much closer to the tip of the root upon ethylene treatment (Le et al., 2001). We conclude that ethylene targets the most rapid phase of cell expansion when the signal is able to exert maximal control over root growth.

Ethylene Is Dependent on Auxin for Maximal Inhibition of Root Cell Expansion

The signal transduction pathway that mediates ethylene inhibition of root growth is usually displayed as a linear sequence of events involving first ethylene and then auxin signaling components (Roman et al., 1995). However, our growth measurements suggest that ethylene can also inhibit root growth independently of auxin. For example, ethylene is still able to cause ~20% reduction in *aux1* root growth (Figure 5). Stepanova et al. (2007) have observed that the ethylene-responsive reporter *EBS:GUS* is expressed in two spatially distinct groups of root cells, suggesting that several sites of ethylene action exist in the root. The first group of *EBS:GUS*-expressing cells at the root apex colocalizes with the site of ethylene-responsive auxin biosynthesis (Stepanova et al., 2005). The second group of *EBS:GUS*-expressing root cells colocalizes with the region of the elongation zone most affected by ACC treatment in our kinematic studies (Figure 5).

Intriguingly, Stepanova et al. (2007) observed that *EBS:GUS* expression in elongation zone cells is dependent on auxin since ethylene was no longer able to induce reporter activity in an *aux1* mutant background. Rahman et al. (2001) elegantly demonstrated that *aux1* root growth could be sensitized toward ethylene when cultured in the presence of auxin. Ethylene appears to require auxin to cause maximal inhibition of cell expansion. For example, 1 μM ACC can cause a 50% inhibition of cell expansion in wild-type roots, yet the same concentration of ACC reduced *aux1* cell expansion by only 20% (Figure 4). An explanation for the requirement of auxin by ethylene to inhibit cell expansion may be provided by the recent transcriptomic results of Stepanova et al. (2007). The authors observed that transcripts encoding cell wall proteins were significantly enriched among genes coregulated by auxin and ethylene. These coregulated genes may encode proteins that effect critical changes to the cell wall of elongation zone cells that are necessary to cause growth inhibition. De Cnodder et al. (2005) recently highlighted the functional importance of Hyp-rich glycoprotein cross-linking during ACC-induced inhibition of root cell expansion. Hyp-rich glycoproteins become cross-linked via intramolecular isodityrosine bridges (Epstein and Lamport, 1984). De Cnodder et al. (2005) observed that addition of external Tyr significantly reduced the growth inhibitory effect of ACC. Intramolecular isodityrosine bridges are catalyzed by hydrogen peroxide (Brady and Fry, 1997). De Cnodder et al. (2005) detected a burst of apoplastic reactive oxygen species in elongation zone cells following ACC treatment. Hence, ACC appears to rapidly inhibit root cell expansion by inducing a series of apoplastic chemical reactions that promotes cell wall cross-linking (De Paepe et al., 2004).

Irrespective of the molecular mechanisms, there is a clear requirement for auxin to be present in elongation zone tissues for ethylene to inhibit cell expansion. Hence, auxin appears to function as a permissive signal that is required for ethylene action. We propose that ethylene upregulates auxin biosynthesis to enhance its ability to inhibit root growth.

METHODS

IAA Measurements

Columbia seeds were placed on agar plates (50 seeds in two rows/plate; 1% agar, 1% sucrose, and 1× MS, pH 5.7, vernalized for 3 d, and incubated in vertical position in long days (16 h light/8 h darkness), with a light intensity of 150 μEinsteins and a temperature of 23°C. For experiments designed to test the effect of elevating the level of the ethylene precursor ACC on the rate of IAA biosynthesis (Figure 1A), 6-d-old seedlings were incubated in liquid medium containing 30% D_2O, 1% sucrose, 1× MS, pH 5.7 ± 1, and 10 μM ACC for 12 and 24 h. Ten seedlings were pooled and weighed for each sample. All samples were analyzed in triplicates as described by Ljung et al. (2005). $^{13}C_6$-IAA (500 pg) was added to each sample as an internal standard. For experiments designed to test the effect of inhibiting ethylene biosynthesis on the rate of IAA biosynthesis and IAA abundance (Figure 1A), 6-d-old seedlings were incubated in liquid medium containing 30% D_2O, 1% sucrose, 1× MS, pH 5.7 ± 1, and 10 μM AVG for 12 and 24 h. Ten seedlings were pooled and weighed for each sample. All samples were analyzed in triplicates as described by Ljung et al. (2005). $^{13}C_6$-IAA (500 pg) was added to each sample as an internal standard. For experiments designed to test the effect of inhibiting ethylene biosynthesis on the rate of IAA biosynthesis in root apical tissues, 6-d-old intact seedlings or excised roots (Figure 1B) were incubated in liquid medium containing 30% D_2O, 1% sucrose, 1× MS, pH 5.7 ± 1, or 10 μM AVG for 24 h. The root tip was collected in 2 × 2-mm sections. One hundred 2-mm sections were pooled for each sample. All samples were analyzed in triplicates as described by Ljung et al. (2005). $^{13}C_6$-IAA (250 pg) was added to each sample as an internal standard. For calculation of the relative synthesis rate of IAA (t/t-ratio), enrichment is expressed as the ratio of deuterium-labeled IAA (tracer) to unlabeled IAA (tracee), after correction for natural isotope distribution to m/z of 203, 204, and 205. Control samples were incubated without ^2H_2O in the medium and analyzed to correct for possible background from the sample matrix. For calculation of IAA concentration, the amount of endogenous IAA in the samples was quantified by combining the corrected areas of the ions from deuterium-labeled IAA (m/z 203 to 205) with that of unlabeled IAA (m/z 202).

Characterization of Mutant and Transgenic Plant Material

Arabidopsis thaliana seedlings were grown according to Swarup et al. (2005). For ethylene treatment, 4-d-old seedlings were placed in air-tight gas jars in the presence of 10 μL/L ethylene for 48 h. GUS assays were performed as described by Malamy and Benfey (1997). GUS-stained seedlings were viewed using differential interference contrast optics as described by Malamy and Benfey (1997).

Kinematic Analysis

Seedlings were surface sterilized with 15% sodium hypochloride for 10 min. For root growth analyses, they were plated on 12 × 12-cm^2 Petri dishes containing 50 mL of an agar-solidified, 0.5× MS micro- and macronutrient solution (Duchefa) with 0.1% sucrose and 0.8% plant tissue culture agar (Lab M). The plates were sealed with Urgopore tape (Laboratoire Urgo) and kept for 3 d at 4°C and then (at day 0) placed at an inclination of ~85° in a growth chamber under constant conditions (22°C and 80 μmol m^{-1} s^{-1} of light supplied by a set of cool white influorescent tubes).

For measurements of the strain rate profile, the plates were placed vertically on the stage of an Axiolab microscope (Zeiss) that was mounted horizontally in the growth chamber so as to have minimal effect on growth conditions during the observation. A series of sequential image stacks spanning 3 to 4 mm of the tip of each root was digitized through the lid of the plate. Each stack contained nine images taken at 30-s intervals. A long-working-distance lens (Epiplan, ×10, numerical aperture = 0.20; Zeiss) and an imaging system encompassing a CCD camera (4910 CCIR; Cohu) and frame grabber board (LG3 CCIR; Scion) was mounted in a Pentium II PC running the image analysis program Scion Image (WinNT version β3b). The obtained image sequences were then analyzed using RootflowRT (van der Weele et al., 2003). Subsequently, the data were smoothed and interpolated into 25-μm-spaced data points using a kernel-smoothing routine described earlier (Beemster and Baskin, 1998) implemented as a macro in Microsoft Excel (version 97). This routine also calculated the derivative of the fitted function ($\delta v/\delta x$) that equals the local relative rate of cell expansion [$r(x)$].

The cell length profile of epidermal (trichoblasts and atrichoblasts) and cortical cells was subsequently determined from the same roots that were stained with propidium iodine, whole mounted, and imaged with a confocal microscope (Zeiss; LSM500) at ×20. The length of all cells in a file of a given cell type was then measured using the public domain image analysis software ImageJ (http://rsb.info.nih.gov/ij/). The position of each cell was calculated from the cumulative length of all cells between it and the quiescent center. Subsequently, the data were smoothed and interpolated into 25-μm-spaced data points using a kernel-smoothing routine described earlier (Beemster and Baskin, 1998) implemented as a macro in Microsoft Excel (version 97), allowing the calculation of averages and standard errors between replicate roots.

qRT-PCR Analysis of Auxin and Ethylene-Responsive Gene Expression

Vertically grown 10-d-old *Arabidopsis* seedlings (Col-0 and *aux1-22*) were treated with 2 ppm ethylene for 3, 6, or 15 h, or with ethylene-free air for the same time periods as a control. Whole roots were frozen in liquid nitrogen for further RNA extraction at the end of the treatment. Treatments were done in triplicates (biological repeats). Total RNA was extracted using Trizol reagent (Gibco BRL), and 5 μg of RNA was further purified and concentrated using the DNA-free RNA kit (Zymo Research) according to the manufacturer's protocols. Purified RNA concentration was quantified with Ribo-Green (Molecular Probes) on a Victor2 fluorometer (Perkin-Elmer), and cDNA was synthesized from 2 μg of total RNA with the RevertAid H Minus first-strand cDNA synthesis kit (Fermentas).

Primers were designed using Beacon Designer 4.0 software from Premier Biosoft International. Primers used were as follows: *IAA1* forward, 5′-ACAATCCCAAGAAGAGCAATAAC-3′, and reverse, 5′-CTCACTATACTTTAACGGAGAAGC-3′; *ERF1* forward, 5′-GACGGAGAATGACCAATAAGAAG-3′, and reverse, 5′-CCCAAATCCTCAAAGACAACTAC-3′; and *APT1* forward, 5′-TTCTCGACACTGAGGCCTTT-3′, and reverse, 5′-TAGCTTCTTGGGCTTCCTCA-3′.

qRT-PCR was performed using a Cybergreen fluorescence-based assay kit (Platinum SYBR Green qPCR kit; Invitrogen) according to the manufacturer's instructions. The PCR reactions were performed on a Rotor-Gene 2000 real-time cycler from Corbett Research, and data were analyzed using the manufacturer's software (Rotor Gene 6). PCR reactions were performed with 500 nM of each primer in a 25-μL reaction under the following conditions: 50°C for 2 min followed by 45 three-step cycles at 95°C for 15 s, 56°C for 30 s, and 72°C for 30 s. All mRNA levels were calculated from threshold cycle values, relative to control treatments, and normalized with respect to housekeeping transcript levels of adenine phosphoribosyltransferase1 (*Apt1*) according to Pfaffl (2001). All samples were run in duplicates (technical repeats). Data represent the average of three biological repeats.

Supplemental Data

The following materials are available in the online version of this article.

Supplemental Figure 1. Ethylene Signaling Mutants ctr1 and ein2 Modify the Expression of the Auxin-Responsive Reporter $IAA2_{pro}$:*GUS*.

Supplemental Figure 2. The Partial Loss-of-Function Allele *aux1-2* Exhibits Ethylene-Sensitive Root Growth.

Supplemental Figure 3. Tissue-Specific GAL4 Driver Lines Were Used to Target axr3-1 Expression to Disrupt Auxin Responses in Selected Root Cell Types.

Supplemental Figure 4. Disrupting Auxin Responses in Elongation Zone Tissues Confers Ethylene-Insensitive Root Growth.

Supplemetal Figure 5. Targeting axr3-1 Expression in Elongation Zone Tissues Confers Ethylene-Resistant Root Growth.

ACKNOWLEDGMENTS

We thank the Nottingham Arabidopsis Stock Centre, Joe Ecker, Billy Sinclair, Fernan Federici, and Jim Haseloff for kindly providing seed used in this study. We also thank Jose Alonso, Anna Stepanova, Eva Benkova, Graham Seymour, and members of the Bennett laboratory for helpful discussions about the work. We acknowledge the support of the Biotechnology and Biological Science Research Council and the Engineering and Physical Sciences Research Council Centres for Integrative Systems Biology Program (M.J.B.), European Union Training Site Grant HTMC-CT-2000-00088 awarded to Plant Systems Biology (P.P. and G.T.S.B.), the fund for Scientific Research-Flanders (D.V.D.S.), the Gatsby Charitable Foundation (M.J.B.), the Swedish Research Council and the Swedish Foundation for Strategic Research (G.S., R.B., and K.L.), and the Interuniversity Poles of Attraction Program-Belgian Science Policy (P6/33).

Received April 5, 2007; revised June 12, 2007; accepted June 18, 2007; published July 13, 2007.

REFERENCES

Abel, S., and Theologis, A. (1995). A polymorphic bipartite motif signals nuclear targeting of early auxin-inducible proteins related to Ps-IAA4 from pea (*Pisum sativum*). Plant J. **8:** 87–96.

Alonso, J.M., and Stepanova, A.N. (2004). The ethylene signaling pathway. Science **306:** 1513–1515.

Alonso, J.M., Stepanova, A.N., Solano, R., Wisman, E., Ferrari, S., Ausubel, F.M., and Ecker, J.R. (2003). Five components of the ethylene-response pathway identified in a screen for weak ethylene-insensitive mutants in Arabidopsis. Proc. Natl. Acad. Sci. USA **100:** 2992–2997.

Beemster, G.T.S., and Baskin, T.L. (2000). STUNTED PLANT 1 mediates effects of cytokinin, but not of auxin, on cell division and expansion in the root of Arabidopsis. Plant Physiol. **124:** 1718–1727.

Beemster, G.T.S., and Baskin, T.I. (1998). Analysis of cell division and elongation underlying the developmental acceleration of root growth in *Arabidopsis thaliana*. Plant Physiol. **116:** 1515–1526.

Brady, D.J., and Fry, S.C. (1997). Formation of di-siodityrosine and loss of isodityrosine in the cell walls of tomato cell-suspension cultures treated with fungal elicitors and H_2O_2. Plant Physiol. **115:** 87–92.

Chang, C., Kwok, S.F., Bleecker, A.B., and Meyerowitz, E.M. (1993). Arabidopsis ethylene-response gene ETR1: Similarity of product to two-component regulators. Science **262:** 539–544.

Chaves, A.L.S., and de Mello-Farias, P.C. (2006). Ethylene and fruit ripening: From illumination gas to the control of gene expression, more than a century of discoveries. Genet. Mol. Biol. **29:** 508–515.

Chilley, P.M., Casson, S.A., Tarkowski, P., Wang, K.L.-C., Hawkins, N., Hussey, P.J., Beale, M., Ecker, J.R., Sandberg, G.K., and Lindsey, K. (2006). The POLARIS peptide of *Arabidopsis* regulates auxin transport and root growth via effects on ethylene signaling. Plant Cell **18:** 3058–3072.

Clark, D.G., Gubrium, E.K., Barrett, J.E., Nell, T.A., and Klee, H.J. (1999). Root formation in ethylene-insensitive plants. Plant Physiol. **121:** 53–59.

Clark, K.L., Larsen, P.B., Wang, X., and Chang, C. (1998). Association of the *Arabidopsis* CTR1 Raf-like kinase with the ETR1 and ERS ethylene receptors. Proc. Natl. Acad. Sci. USA **95:** 5401–5406.

De Cnodder, T., Vissenberg, K., Van Der Straeten, D., and Verbelen, J.-P. (2005). Regulation of cell length in the *Arabidopsis thaliana* root by the ethylene precursor 1-aminocyclopropane-1-carboylic acid: A matter of apoplastic reactions. New Phytol. **168:** 541–550.

De Paepe, A., Vuylsteke, M., Van Hummelen, P., Zabeau, M., and Van Der Straeten, D. (2004). Transcriptional profiling by cDNA-AFLP and microarray analysis reveals novel insights into the early response to ethylene in *Arabidopsis*. Plant J. **39:** 537–559.

Dharmasiri, S., Swarup, R., Mockaitis, K., Dharmasiri, N., Singh, S.K., Kowalchyk, A., Marchant, A., Mills, S., Sandberg, G., Bennett, M.J., and Estelle, M. (2006). AXR4 is required for localization of the auxin influx facilitator AUX1. Science **312:** 1218–1220.

Epstein, L., and Lamport, D.T.A. (1984). An intramolecular linkage involving isodityrosine in extensin. Phytochemistry **23:** 1241–1246.

Hobbie, L., and Estelle, M. (1995). The axr4 auxin resistant mutants of *Arabidopsis* thaliana define a gene important for root gravitropism and lateral root initiation. Plant J. **7:** 211–220.

Hussain, A., Black, C.R., Taylor, I.B., and Roberts, J.A. (1999). Soil compaction. A role for ethylene in regulating leaf expansion and shoot growth in tomato? Plant Physiol. **121:** 1227–1237.

Hussain, A., and Roberts, J.A. 2002. Role of ethylene in coordinating root growth and development. In Plant Roots: The Hidden Half, Y. Waisel, A. Eshel, and U. Kafkafi, eds (New York: Marcel Dekker), pp. 449–459.

Kieber, J.J., Rothenberg, M., Roman, G., Feldmann, K.A., and Ecker, J.R. (1993). CTR1, a negative regulator of the ethylene response pathway in Arabidopsis, encodes a member of the raf family of protein kinases. Cell **72:** 427–441.

Le, J., Vandenbussche, F., Van Der Straeten, D., and Verbelen, J.P. (2001). In the early response of *Arabidopsis* roots to ethylene, cell elongation is up and down regulated and uncoupled from differentiation. Plant Physiol. **125:** 519–522.

Leyser, H.M.O., Pickett, F.B., Dharmasiri, S., and Estelle, M. (1996). Mutations in the AXR3 gene of *Arabidopsis* result in altered auxin response including ectopic expression from the SAUR-AC1 promoter. Plant J. **10:** 403–413.

Ljung, K., Hull, A.K., Celenza, J., Yamada, M., Estelle, M., Normanly, J., and Sandberg, G. (2005). Sites and regulation of auxin biosynthesis in *Arabidopsis* roots. Plant Cell **17:** 1090–1104.

Luschnig, C., Gaxiola, R.A., Grisafi, P., and Fink, G.R. (1998). EIR1: A root specific protein involved in auxin transport, is required for gravitropism in *Arabidopsis thaliana*. Genes Dev. **12:** 2175–2187.

Malamy, J.E., and Benfey, P.N. (1997). Organization and cell differentiation in lateral roots of *Arabidopsis thaliana*. Development **124:** 33–44.

Masucci, J.D., and Schiefelbein, J.W. (1996). Hormones act downstream of TTG and GL2 to promote root hair outgrowth during epidermis development in the *Arabidopsis* root. Plant Cell **8:** 1505–1517.

Pickett, F.B., Wilson, A.K., and Estelle, M. (1990). The aux1 mutation of *Arabidopsis* confers both auxin and ethylene resistance. Plant Physiol. **94:** 1462–1466.

Pfaffl, M.W. (2001). A new mathematical model for relative quantification in real-time PCR. Nucleic Acids Res. **29:** 2002–2007.

Rahman, A., Amakawa, T., Goto, N., and Tsurumi, S. (2001). Auxin is a positive regulator for ethylene-mediated response in the growth of *Arabidopsis* roots. Plant Cell Physiol. **42:** 301–307.

Roman, G., Lubarsky, B., Kieber, J.J., Rothenberg, M., and Ecker, J.R. (1995). Genetic analysis of ethylene signal transduction in *Arabidopsis thaliana*: Five novel mutant loci integrated into a stress response pathway. Genetics **139:** 1393–1409.

Růžička, K., Ljung, K., Vanneste, S., Podhorská, R., Beeckman, T., Friml, J., and Benková, E. (2007). Ethylene regulates root growth through effects on auxin biosynthesis and transport-dependent auxin distribution. Plant Cell **19:** 2197–2212.

Smalle, J., and Van Der Straeten, D. (1997). Ethylene and vegetative development. Physiol. Plant **100:** 593–605.

Solano, R., Stepanova, A., Chao, Q., and Ecker, J.R. (1998). Nuclear events in ethylene signaling: a transcriptional cascade mediated by ETHYLENE-INSENSITIVE3 and ETHYLENE-RESPONSE-FACTOR1. Genes Dev. **12:** 3703–3714.

Stepanova, A.N., and Alonso, J.M. (2005). Ethylene signaling and response pathway: A unique signaling cascade with multiple inputs and output. Physiol. Plant. **123:** 195–206.

Stepanova, A.N., Hoyt, J.M., and Hamilton, A.A. (2005). A link between ethylene and auxin uncovered by the characterization of two root-specific ethylene-insensitive mutants in Arabidopsis. Plant Cell **17:** 2230–2242.

Stepanova, A.N., Yun, J., Likhacheva, A.V., and Alonso, J.M. (2007). Multilevel interactions between ethylene and auxin in *Arabidopsis* roots. Plant Cell **19:** 2169–2185.

Swarup, R., Friml, J., Marchant, A., Ljung, K., Sandberg, G., Palme, K., and Bennett, M.J. (2001). Localization of the auxin permease AUX1 suggests two functionally distinct hormone transport pathways operate in the *Arabidopsis* root apex. Genes Dev. **15:** 2648–2653.

Swarup, R., et al. (2004). Structure-function analysis of the presumptive *Arabidopsis* auxin permease AUX1. Plant Cell **14:** 3069–3083.

Swarup, R., Kramer, E.M., Perry, P., Knox, K., Leyser, H.M.O., Haseloff, J., Beemster, G.T.S., Bhalerao, R., and Bennett, M.J. (2005). Root gravitropism requires lateral root cap and epidermal cells for transport and response to a mobile auxin signal. Nat. Cell Biol. **7:** 1057–1065.

Swarup, R., Parry, G., Graham, N., Allen, T., and Bennett, M.J. (2002). Auxin cross-talk: integration of signalling pathways to control plant development. Plant Mol. Biol. **49:** 411–426.

Tanimoto, M., Roberts, K., and Dolan, L. (1995). Ethylene is a positive regulator of root hair development in *Arabidopsis thaliana*. Plant J. **8:** 943–948.

Timpte, C., Lincoln, C., Pickett, F.B., Turner, J., and Estelle, M.A. (1995). The *AXR1* and *AUX1* genes of *Arabidopsis* function in separate auxin-response pathways. Plant J. **8:** 561–569.

van der Weele, C.M., Jiang, H.S., Palaniappan, K.K., Ivanov, V.B., Palaniappan, K., and Baskin, T.I. (2003). A new algorithm for computational image analysis of deformable motion at high spatial and temporal resolution applied to root growth. Roughly uniform elongation in the meristem and also, after an abrupt acceleration, in the elongation zone. Plant Physiol. **132:** 1138–1148.

Wilson, A.K., Pickett, F.B., Turner, J.C., and Estelle, M. (1990). A dominant mutation in *Arabidopsis* confers resistance to auxin, ethylene and abscisic acid. Mol. Gen. Genet. **222:** 377–383.

Wisniewska, J., Xu, J., Seifertová, D., Brewer, P.B., Růžička, K., Blilou, I., Rouquié, D., Benková, E., Scheres, B., and Friml, J. (2006). Polar PIN localisation directs auxin flow in plants. Science **312:** 883.

Yang, Y.D., Hammes, U.Z., Taylor, C.G., Schachtman, D.P., and Nielsen, E. (2006). High-affinity auxin transport by the AUX1 influx carrier protein. Curr. Biol. **16:** 1123–1127.